

Aggregation-Induced Emission of Naphthalene Diimides: Effect of Chain Length on Liquid and Solid-Phase Emissive Properties

Alberto Insuasty⁺,^[a, b] Serena Carrara⁺,^[c] Jiao Xuechen,^[d] Christopher R. McNeill,^[d] Conor Hogan,^[c] and Steven J. Langford^{*[a, e]}

The aggregation-induced emission (AIE) properties of a systematic series of naphthalene diimides (NDIs) varying the chain length at the imide positions have been studied. A solvophobic collapse of NDI units through the flash injection of THF NDI solutions in sonicating water triggers the formation of stable suspensions with enhanced fluorescence emissions. Shorter chains favor the π - π stacking of NDI units through H-

aggregation producing a strong AIE effect showing remarkably high quantum yields that have not been observed for non core-substituted NDIs previously. On the other hand, NDIs functionalized with longer chains lead to more disordered domains where π - π stacking between NDI units is mainly given by *J*-aggregation unfavoring the AIE effect.

Introduction

Naphthalene diimides (NDIs) have been extensively studied for many years due to their exceptional electronic properties. NDIs are planar and electron deficient molecules exhibiting high electron affinities and capability to self-assemble to form higher nanoarchitectures, which make them good candidates for a broad range of several applications such as supramolecular chemistry, molecular recognition, biological sensors, bioimaging

and optoelectronic devices.^[1–6] The chemical versatility of NDIs, synthetically speaking, offers the possibility to functionalize them mainly at the core or the imide positions, giving rise to large library of molecules with tunable electronic properties, good charge carrier mobilities, remarkable thermal and oxidative stabilities, which make NDI units excellent building blocks for applications in photovoltaic devices and flexible displays.^[7,8] The functionalization on the naphthalene core (via core-substitution or core annulation), mostly with heteroatoms (N, S, O) can affect dramatically their electronic properties producing a range of compounds with almost a palette of custom designed colors with moderate or good quantum yields.^[3,9,10] The functionalization at the imide nitrogens (*N*-imide), affects not only their solubility, but also the supramolecular packing and even the processability in optoelectronic devices where different organized layers are desirable.^[11–13] However, the application of non core-substituted NDI in fluorescence sensing or light emitting have been hindered due to their weak fluorescent quantum yields.^[10]

In the last decade, the Aggregation-Induced Emission (AIE) phenomena has attracted a large interest since it is well manifested in self-aggregating materials.^[14–16] This phenomena has emerge as a new concept that changes the reasoning of scientists in regard to classical photophysical features. In the AIE effect the emission fluorescence properties is enhanced and allow these molecules to exhibit more efficient light emission when they aggregate usually through π - π contributions. The mechanisms that lead to AIE effect, firstly elucidated by Tang *et al.*,^[16–18] are related to a process called restricted intramolecular motions (RIM), which can be obtained for instance through self-aggregation, solid state, hydrophilic interactions and excimer formation. In particular, the phenomenon has been exploited for applications in bioimaging and theragnostic due to the excellent photostability of such aggregates and high fluorescence quantum yields.^[19–22] AIE phenomena can also

[a] Dr. A. Insuasty,⁺ Prof. S. J. Langford
 Department of Chemistry and Biotechnology
 Swinburne University of Technology
 Hawthorn, VIC 3122 (Australia)

[b] Dr. A. Insuasty⁺
 Grupo de Investigación de Compuestos Heterocíclicos
 Departamento de Química
 Universidad del Valle
 Calle 13 # 100-00, Cali 760032 (Colombia)

[c] Dr. S. Carrara,⁺ Prof. C. Hogan
 La Trobe Institute for Molecular Science
 La Trobe University
 Melbourne, VIC 3086 (Australia)

[d] Dr. J. Xuechen, Prof. C. R. McNeill
 Department of Materials Science and Engineering
 Monash University
 Melbourne, VIC 3080 (Australia)

[e] Prof. S. J. Langford
 School of Mathematical and Physics Sciences
 University of Technology Sydney
 Ultimo, NSW 2007 (Australia)
 E-mail: steven.langford@uts.edu.au

[⁺] Equal contribution.

Supporting information for this article is available on the WWW under <https://doi.org/10.1002/asia.202400152>

© 2024 The Authors. Chemistry - An Asian Journal published by Wiley-VCH GmbH. This is an open access article under the terms of the Creative Commons Attribution Non-Commercial NoDerivs License, which permits use and distribution in any medium, provided the original work is properly cited, the use is non-commercial and no modifications or adaptations are made.

bring a wide range of opportunities in sensing,^[23] nanomedicine^[24] and organic solar cells.^[25]

The AIE effect has been observed on NDIs derivatives with great ability to self-organize in supramolecular assemblies upon different stimuli such as solvent effects, temperature and condensed states.^[1,26–29] Core-substituted NDIs (cNDIs) with high tendency to self-assemble and exhibiting AIE effect have been reported and studied in several occasions.^[27,30–32] Simple NDIs functionalized only at imide positions have also exhibited AIE phenomena. Among the latter, various cases usually requires the non-symmetric functionalization at the imide positions. For instance, electron-donor units and aliphatic chains moieties at the imide positions, are able to self-assemble through amide H-bonding, π - π stacking of the NDI cores and hydrophobic interactions between the alkyl chains, which can be balanced by solvophobic control using different mixture of solvents.^[33] However, such supramolecular ensembles tends to exhibit an AIE effect with moderate photoluminescence quantum yields (ϕ_{PL}), together with the need of relatively long synthetic procedures to obtain the unsymmetrical NDI derivatives.

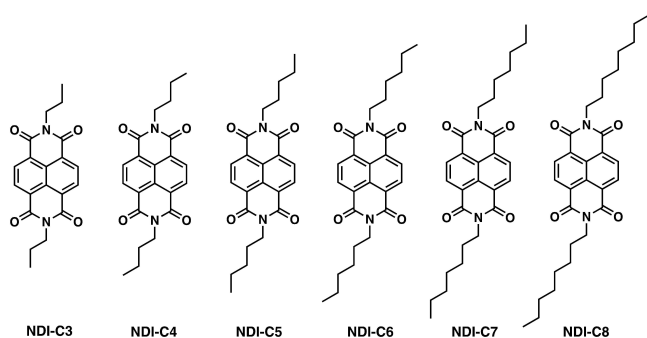


Figure 1. Molecular structures of NDIs varying the chain length, from the left NDI-C3 to the right NDI-C8.

Regarding the symmetrical functionalization at the imide positions we have previously reported simple NDIs whose optical properties were switched on through the melt of crystalline materials to demonstrate how macromolecular order effects optical brightness.^[28] Symmetrical NDIs with long chains have been also reported exhibiting AIE effects but still relatively low quantum yields are observed.^[34–36]

Here, we present a systematic case study using NDIs with varying the length of the chains at imide positions (Figure 1) evaluating the effect on the emissive properties at the liquid and solid-phase. The synthesis is a one-step reaction through the commercially-available naphthalene dianhydride with C3–C8 amines (see supporting information). Although some studies of the effect of elongating the chains in NDIs have been performed, they have been devoted to study their supramolecular structures on highly oriented pyrolytic graphite (HOPG) surfaces,^[37] thermal expansion behavior on thin films^[38] and field-effect transistors,^[39] but none have focused their attention on the study of AIE behavior. We demonstrate how elongating chains at the imide position can bring a change in the emission properties in an aggregated form in the liquid and solid states, allowing quantification through a color palette used in several applications.

Results and Discussion

Absorption studies of all compounds NDI-(C3–C8) in THF (solvent in which NDI molecules are well solvated) across the UV-Vis range exhibited the characteristic bands in the near-UV at 380, 360 and 340 nm related to the π - π^* transitions polarized along the long axis of the NDI (Figure 2A).^[40,41] The emission spectra generated from THF solutions upon excitation ($\lambda_{exc} = 340, 360$ or 380 nm) show maxima at 410 nm with a shoulder

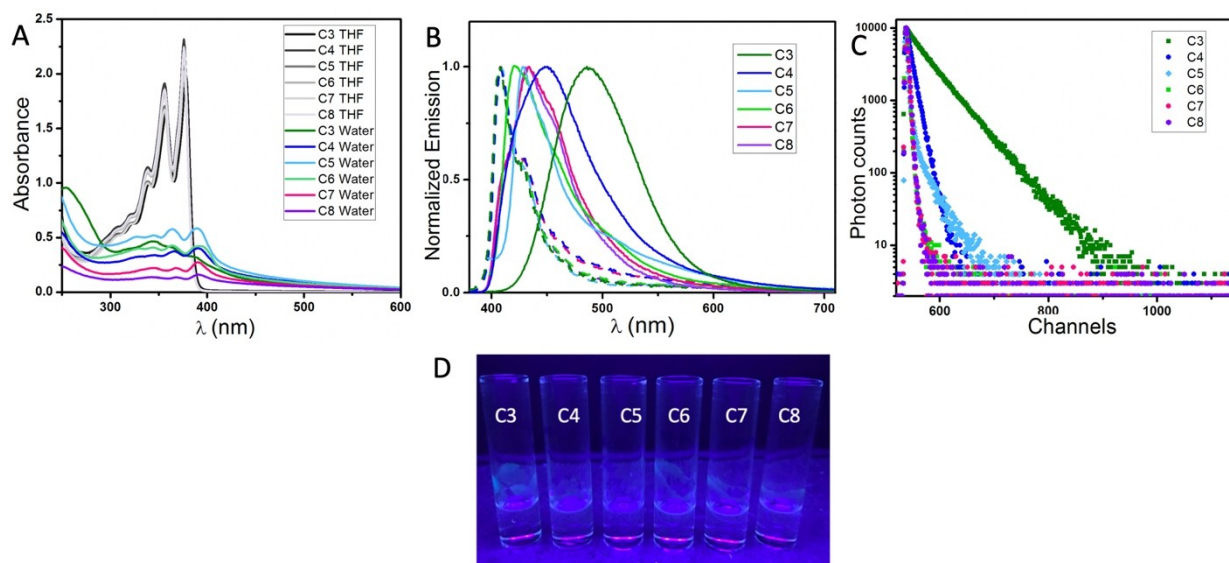


Figure 2. A) Absorption spectra of NDI-(C3–C8) in THF (1×10^{-4} M) and the mixture H₂O:THF (95:5). B) Emission spectra of NDI-(C3–C8) in THF at $\lambda_{exc} = 340, 360, 380$ nm (1×10^{-4} M) (dashed lines) and in the mixture H₂O:THF (95:5) (solid lines). C) Fluorescence lifetime decay profile ($\lambda_{exc} = 344$ nm) of the flash injected solutions in water for NDI-(C3–C8). D) Images of NDI-(C3–C8) in THF under 365 nm hand-lamp irradiation.

around 430 nm, which is usually assigned to the characteristic emission of the NDI core (Figure 2B, dashed lines).^[41] Typically, NDI solutions in THF usually produce a low emissive solutions under 365 nm UV-lamp (Figure 2D). However, it is possible to trigger a nanoprecipitation of NDI units by flash injecting an aliquot of NDI THF solution in sonicating water (see SI for more details), giving rise to a suspension of aggregates showing a marked enhanced emission under the exposure to a UV-lamp illuminated at 365 nm (Figure 3A), thus indicating that NDI-(C3-C8) exhibit an AIE phenomena upon nanoprecipitation in water. This procedure has been used in other reports and represents an efficient methodology to achieve Aggregated-Induced Electroluminescence (AIECL) phenomena in metallic compounds.^[42] UV-vis spectra for NDI-(C3-C8) suspensions showed, on one hand, that for compounds NDI-(C4-C8) a decrease in absorbance and a bathochromic shift with a loss on the fine featuring bands observed in THF to 395, 370 and 345 nm (Figure 2A), commensurate with the formation of *J*-aggregates.^[33,35,43-46] On the other hand, interestingly, the absorption spectra for NDI-C3 suspension (Figure 2A, dark green line), interestingly, shows a different behavior with

respect to the others, exhibiting a blue shifting, displaying the highest absorption peak at 345 nm over absorptions at longer wavelengths, attesting the formation of H-aggregates.^[35,41,48-50] The change in structure within the aggregates prompted us to investigate the vibronic peak ratio 0-0/0-1 for all spectra: NDI-C3 is < 1 indicating the dominance of H-type aggregation, ~1 for intermediate lengths like for NDI-(C4-C6) and becomes > 1 for the longer chains in NDI-(C7 and C8) indicative of the dominance of *J*-type aggregates.^[36,45,50] Obviously, the competition between dispersive forces within this simple series highlights practical design features one can use to produce designer properties.

Fluorescence emission spectra in aqueous solutions for all NDI-(C3-C8) derivatives are shown in Figure 2B (solid lines). The emission spectra of all NDI derivatives in aqueous solution showed a bathochromically shifted emission ranging from 420 nm to 500 nm, being more pronounced that shifting and with broader bands in the case of shorter chains such as NDI-C3 and NDI-C4 (Figure 2B). The reason why NDI-C3 and NDI-C4 show broader and featureless bands could be found in the nature of the lowest-energy transition, which is usually dipole-forbidden for H-aggregated but allowed for *J*-aggregates.^[36,51]

The excited-state lifetime decays also show a change passing from THF to water due to the formation of aggregates (Figure 2C, Table 1). H-aggregates of NDIs have shown for similar compounds longer lifetimes than *J*-aggregates, and in contrast with the monomeric dissolved form.^[29,47,52] In this case, it is observed a decrease of lifetime exciting at 344 nm and monitoring at the characteristic emission wavelength of each molecule with the lengthening of the chains. The only monoexponential decay found is the one associated with the excited state of the NDI C3 H-aggregate, which also displays the longest-lived lifetime – all the others examples are multi-exponential and shorter in value (see Table S1 in the supporting information for complete data). This behavior could be attributed to the fact that different intermolecular interactions between neighboring NDI units can give rise to different exciton dynamics, where distinct exciton migration and relaxation processes take place. In this sense, probably, in *J*-aggregates the stacking arrangement of NDI units leads to a splitting of the excitonic energy levels due to the weak intermolecular coupling. This energy splitting results in the presence of multiple excitonic states with different energies and lifetimes. On the other hand, the stacking arrangements in

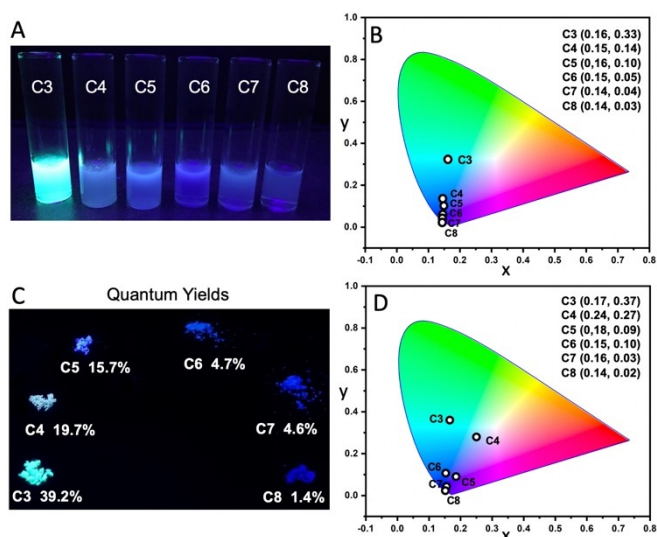


Figure 3. A) Images of the flash injected THF NDI-(C3-C8) solutions in water (H₂O:THF; 95:5) under 365 nm hand-lamp irradiation. B) CIE coordinates of the NDI-(C3-C8) in water suspensions. C) Images of NDI-(C3-C8) in the solid state under 365 nm hand-lamp irradiation. D) CIE coordinates of NDI-(C3-C8) in the solid state.

Table 1. Photophysical properties of NDI C3-C8 in THF, H₂O and solid state (SS). ^a λ_{exc} 340, 360, 380 nm; ^b λ_{exc} 344 nm nanoled light source. ^caverage lifetime (SI for complete data values).

	Emission (nm) ^a		Φ_{PL} (%)	τ_{ave} (ns) ^b		
	λ_{max} THF	λ_{max} H ₂ O		THF	H ₂ O	SS
C3	408	490	< 1	21.9	39.2	< 1
C4	408	450	< 1	14.7	19.7	< 1
C5	408	428	< 1	6.5	15.7	< 1
C6	408	421	< 1	1.5	4.7	< 1
C7	408	434	< 1	< 1	4.6	< 1
C8	408	434	< 1	< 1	1.4	< 1

H-aggregates allow for strong intermolecular interactions, which facilitate efficient exciton migration and energy transfer processes within the aggregate. As a result, the excited-state is effectively channeled towards a dominant decay pathway, leading to a single exponential decay or dominant decay component.^[49,53–56]

It is clear from Figure 3A, that dramatic optical effects are seen across this series. Even to the naked eye, the longer the alkyl chain, the bluer the emission (Figure 3A). CIE coordinates of nanoaggregates solutions in water exhibiting AIE properties show a linear trend in the chromatic diagram (Figure 3B), moving in the blue region from whiter to bluer shifted coordinates commensurate with shorter to longer chains (Figure 3B). To the best of our knowledge, such a behavior stemming from a small and simple set of organic molecules with only a slight modification on the molecular structure have not been observed and should lead to interest in the design of new chromophores with the possibility of linear adjustment of modulated specific emissions. Most of the examples exhibiting such linear behavior are dye-based, metal-coordination polymers or perovskites.^[57–60]

Studies in the solid state of **NDI-(C3–C8)** also display AIE properties (Figure 3C). As depicted in Figure S1 (in the supporting information), emission profiles are broader and less featured than in THF resembling the results described upon nanoprecipitation. Solid state ϕ_{PL} (Figure 3C, Table 1) follow as well the same trend with a decrease in value passing from shorter to longer alkyl chains. This produces a cone pattern on the CIE chromaticity diagram of possible colors that can be modulated by shortening or elongating the alkyl chain of these NDI molecules (Figure 3D). We believe that such a difference between both CIE diagrams rely on the different packing from the solid state to the nanoprecipitated where H-aggregates are more favored in the solid state. The ϕ_{PL} for **NDI-C3** in the solid state (39.2%) is the highest quantum yield so far reported for a non core-substituted NDI, and its ϕ_{PL} obtained in solution (21.9%, Table 1) is one of the highest so far reported for a simple NDI just behind few cases reported.^[33,62] However, in one of those cases the synthesis of NDI derivatives requires up to five reactions steps achieving a non-symmetric functionalization at the *N*-imide positions. The resulting amphiphile molecule is capable of self-assemble into microcapsule nanostructures stabilized via amide H-bonding an exhibiting an AIE effect with a ϕ_{PL} of 22.8%.^[33] In the other example, a chemosensor based on carboxyl functionalized NDI showed AIE after reaction with Hg^{2+} leading to a ϕ_{PL} of 32%.^[61] It is clear that our methodology becomes quite appealing with just one reaction step of synthesis and no metal required or a further functionalization for AIE phenomena. In other examples, NDI units with long saturated and unsaturated alkyl chains at imide position have exhibited AIE effect with quantum yields up to 5% in THF/ H_2O mixtures, however still far from the values reported in this work.^[35]

The chain length dependence aggregation behavior of **NDI-(C3–C8)** molecules has also been evaluated by thermal analysis. Differential Scanning Calorimetry (DSC) scans have been implemented on all NDI derivatives with varying chain length.

As summarized in Figure 4A, the onset temperatures of both melting peak and crystallization peak are revealed to monotonically decrease with chain length, suggesting that shorter chain length enables the formation of different aggregation forms when compared to longer ones. Furthermore, transition enthalpy of both melting and crystallization peaks were extracted from the raw DSC data and represented in Figure 4B (see Figure S2 for raw DSC traces). Note that the sudden drop in enthalpy of **NDI-C6** is due to the formation of polymorphic crystallites or different liquid crystal phases as reported for related systems.^[62]

In order to have an insight about π -stacking of the different NDI units, powder XRD measurements were performed (Figure S3). According to the literature concerning NDI supramolecular nanostructures, interplanar π - π distances are reported to be in the range of $2\theta = 23^\circ$ – 25° ,^[41,43,44,63] such characteristic diffraction peaks are more clearly observed for shorter chains (C3–C5) while for larger (C6–C8) such distances are less pronounced (Figure S3). This behavior is indicative of a supramolecular packing where the π -stacking of NDI units through H-aggregates becomes important, favoring the AIE phenomena with higher quantum yields. The lack of these peaks for longer chains where π - π distances with *J*-aggregates are not so representative rendering the system less emissive.

All the above presented results can be rationalized probably in terms of the degree of freedom of NDI units to stack among the aliphatic chains upon the solvophobic collapse on the flash injection in water. We believe that longer chains with a bigger solvophobic domains leave the NDI cores to interact in a more disordered way favoring *J*-aggregation (Figure 5). On the other hand, shorter chains with a much smaller solvophobic domains constrain NDI cores to stack in a more restricted way (H-

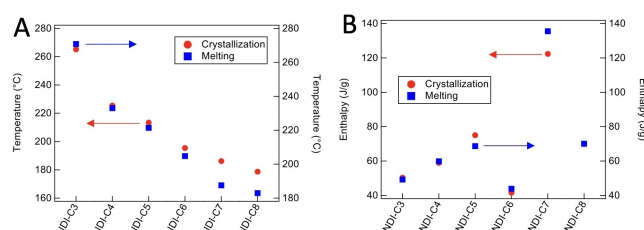


Figure 4. A) Onset temperatures of crystallization and melting peaks as a function of chain length. B) Plots the enthalpy of both crystallization and melting peaks. All values are extracted from primary thermal events with highest temperature for each investigated sample.

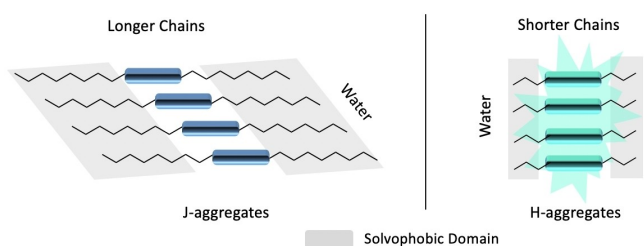


Figure 5. Schematic representation of the possible nanoaggregates showing *J*- and *H*-aggregates upon flash injection in water and exhibiting a marked AIE phenomena for shorter chains.

aggregates) in order to protect NDI cores from water more effectively in which AIE effect is turned on (Figure 5). In this sense, the observed AIE effect is probably given due to the restriction of intramolecular motions as reported elsewhere for non-symmetric NDI systems.^[33] In the aggregated state, the non-radiative decay channels are hindered due to RIM events which lead to the enhancement of emission properties.^[16–18,64]

Conclusions

In conclusion we have studied the AIE properties of simple NDIs varying the length of the alkyl chains (C3–C8). The photo-physical studies of these compounds showed that they assemble into H-type or J-type aggregates depending on the nature of the chain - shorter chains favoured H-aggregates and they are much more emissive in comparison with longer ones exhibiting mainly J-aggregates. A simple synthesis path allowed us to achieve the highest ϕ_{PL} so far reported for simple NDIs in the solid state (C3 – 39.2%) and one of the highest in solution (C3 – 21.9%). Moreover, AIE properties showed a responsive and linear pattern in the chromatic diagram moving from whiter to bluer shifted coordinates when passing from shorter to longer chains, a behavior rarely observed with such a slight modification on a small organic molecule. This here reported strategy together with additional design strategies for bright NDI molecules such as core-substitution or shoulder conjugation, could lead to a wide range of highly emissive molecules for different purposes with relatively ease. H-aggregates could be favored by a solvophobic collapse using short alkyl chains without the need of H-bonds in the molecular self-assembly, which usually requires more complex reaction steps to get the desired molecular structure. We believe that this work paves the way for the design of new NDI molecules as promising AIEgens with simple synthetic strategies.

Acknowledgements

This work was supported by the Australian Research Council (DP170102145 and DP200102947). A.I. gratefully acknowledge Universidad del Valle for the financial support. Open Access publishing facilitated by University of Technology Sydney, as part of the Wiley - University of Technology Sydney agreement via the Council of Australian University Librarians.

Conflict of Interests

The authors declare no conflict of interest.

Data Availability Statement

The data that support the findings of this study are available in the supplementary material of this article.

Keywords: Naphthalene Diimides · Aggregation-Induced Emission · π - π stacking · H-aggregates · J-aggregates

- [1] S. V. Bhosale, M. A. Kobaisi, R. W. Jadhav, P. P. Morajkar, L. A. Jones, S. George, *Chem. Soc. Rev.* **2021**, *50*, 9845–9998.
- [2] S. Kumar, J. Shukla, Y. Kumar, P. Mukhopadhyay, *Org. Chem. Front.* **2018**, *5*, 2254–2276.
- [3] M. Al Kobaisi, S. V. Bhosale, K. Latham, A. M. Raynor, S. V. Bhosale, *Chem. Rev.* **2016**, *116*, 11685–11796.
- [4] M. Sommer, *J. Mater. Chem. C* **2014**, *2*, 3088–3098.
- [5] S. V. Bhosale, C. H. Jani, S. J. Langford, *Chem. Soc. Rev.* **2008**, *37*, 331–342.
- [6] S. L. Suraru, F. Würthner, *Angew. Chem. Int. Ed.* **2014**, *53*, 7428–7448.
- [7] M. A. Jameel, T. C.-J. Yang, G. J. Wilson, R. A. Evans, A. Gupta, S. J. Langford, *J. Mater. Chem. A* **2021**, *9*, 27170–27192.
- [8] S. Valero, A. Cabrera-Espinoza, S. Collavini, J. Pascual, N. Marinova, I. Kosta, J. L. Delgado, *Eur. J. Org. Chem.* **2020**, *33*, 5329–5339.
- [9] A. Insuasty, S. Maniam, S. J. Langford, *Chem. Eur. J.* **2019**, *25*, 7058–7073.
- [10] S. Maniam, S. J. Langford, T. Bell, H. Higginbotham, *Chem. Eur. J.* **2019**, *25*, 7044–7057.
- [11] J.-W. Lee, N. Choi, D. Kim, T. N.-L. Phan, H. Kang, T.-S. Kim, B. J. Kim, *Chem. Mater.* **2021**, *33*, 1070–1081.
- [12] Z. Li, Y. Liang, L. Ying, Y. Cao, *Chem. Eng. J.* **2022**, *448*, 137554.
- [13] F. Zhang, Y. Hu, T. Schuettfort, C. Di, X. Gao, C. R. McNeill, L. Thomsen, S. C. B. Mannsfeld, W. Yuan, H. Siringhaus, D. Zhu, *J. Am. Chem. Soc.* **2013**, *135*, 2338–2349.
- [14] Q. Xia, Y. Zhang, Y. Li, Y. Li, Y. Li, Z. Feng, X. Fan, J. Qian, H. Lin, *Aggregate* **2022**, *3*, 1, e152.
- [15] G. R. Suman, M. Pandey, A. S. Chakravarthy, *Mater. Chem. Front.* **2021**, *5*, 1541–1584.
- [16] J. Mei, N. L. C. Leung, R. T. K. Kwok, J. W. Y. Lam, B. Z. Tang, *Chem. Rev.* **2015**, *115*, 11718–11940.
- [17] Y. Hong, J. W. Y. Lam, B. Z. Tang, *Chem. Soc. Rev.* **2011**, *40*, 5361–5388.
- [18] Y. Hong, J. W. Y. Lam, B. Z. Tang, *Chem. Commun.* **2009**, 4332–4353.
- [19] S. Wang, K. Zhou, X. Lyu, H. Li, Z. Qiu, Z. Zhao, B. Z. Tang, *Chem. Biomed. Imaging* **2023**, *1*, 509–521.
- [20] J. Qian, B. Z. Tang, *Chem* **2017**, *3*, 56–91.
- [21] M. Shellaiah, K.-W. Sun, *Biosensors* **2022**, *12*, 550.
- [22] D. Guo, L. Li, X. Zhu, M. Heeney, J. Li, L. Dong, Q. Yu, Z. Gan, X. Gu, L. Tan, *Sci. China Chem.* **2020**, *63*, 1198–1207.
- [23] B. Naskar, A. Dhara, D. Maiti, M. Kukulka, M. P. Mitoraj, M. S. Hooper, C. Prodhan, K. Chaudhuri, S. Goswami, *ChemPhysChem* **2019**, *20*, 1630–1639.
- [24] Z. Li, S. Chen, W. H. Binder, J. Zhu, *ACS Macro Lett.* **2023**, *12*, 1384–1388.
- [25] L. Zeng, L. Zhang, L. Mao, X. Hu, Y. Wie, L. Tan, Y. Chen, *Adv. Opt. Mater.* **2022**, *10*, 2200968.
- [26] P. Lasitha, E. Prasad, *RSC Adv.* **2015**, *5*, 41420–41427.
- [27] A. Rananaware, D. D. La, S. M. Jackson, S. V. Bhosale, *RSC Adv.* **2016**, *6*, 16250–16255.
- [28] T. D. M. Bell, S. V. Bhosale, C. M. Forsyth, D. Hayne, K. P. Ghiggino, J. A. Hutchison, C. H. Jani, S. J. Langford, M. Lee, C. Woodward, *Chem. Commun.* **2010**, *46*, 4881–4883.
- [29] M. Kumar, S. J. George, *Chem. Eur. J.* **2011**, *17*, 11102–11106.
- [30] H. Long, D. Guo, L. Wang, Z. Liu, S. Li, X. Liang, Y. Chen, Z. Yang, J. Li, L. Dong, L. Tan, *Dyes Pigm.* **2022**, *203*, 110330.
- [31] X. Fang, H. Ke, L. Li, M.-J. Lin, *Dyes Pigm.* **2017**, *145*, 469–475.
- [32] L. Zong, Y. Xie, C. Wang, J. R. Li, Q. Li, Z. Li, *Chem. Commun.* **2016**, *52*, 11496–11499.
- [33] N. V. Ghule, D. D. La, R. S. Bhosale, M. Al Kobaisi, A. M. Raynor, S. V. Bhosale, S. V. Bhosale, *ChemistryOpen* **2016**, *5*, 157–163.
- [34] M. Kumar, S. George, *Nanoscale* **2011**, *3*, 2130.
- [35] P. Lasitha, *ChemistrySelect* **2021**, *6*, 7936–7943.
- [36] P. Choudhury, K. Das, P. K. Das, *Langmuir* **2017**, *33*, 4500–4510.
- [37] Y. Miyake, T. Nagata, H. Tanaka, M. Yamazaki, M. Ohta, *ACS Nano* **2012**, *6*, 3876–3887.
- [38] X. Jiao, S. Maniam, S. J. Langford, C. R. McNeill, *Phys. Rev. Mater.* **2019**, *3*, 013606.
- [39] D. Chlebosz, W. Goldeman, K. Janus, M. Szuster, A. Kiersnowski, *Molecules* **2023**, *28*, 2940.
- [40] M. Brzostowska, K. Kacprzak, H. Kołbon, *Chirality* **2000**, *12*, 263–268.
- [41] H. Shao, J. R. Parquette, *Chem. Commun.* **2010**, *46*, 4285–4287.
- [42] S. Carrara, A. Aliprandi, C. H. Hogan, L. D. Cola, *J. Am. Chem. Soc.* **2017**, *139*, 14605–14610.
- [43] P. Rajdev, M. R. Molla, S. Ghosh, *Langmuir* **2014**, *30*, 1969–1976.

- [44] M. R. Molla, D. Gehrig, L. Roy, V. Kamm, A. Paul, *Chem. Eur. J.* **2014**, *20*, 760–771.
- [45] M. Más-Montoya, R. A. J. Janssen, *Adv. Funct. Mater.* **2017**, *27*, 1605779.
- [46] E. Castellanos, R. M. Gomila, R. Manha, G. Fernandez, A. Frontera, B. Soberats, *J. Mater. Chem. C* **2023**, *11*, 10884–10892.
- [47] S. Basak, N. Nandi, K. Bhattacharyya, A. Datta, A. Banerjee, *Phys.Chem. Chem.Phys.* **2015**, *17*, 30398.
- [48] F. Billeci, F. D'Anna, S. Marullo, R. Noto, *RSC Adv.* **2016**, *6*, 59502.
- [49] A. T. Haedler, K. Kreger, A. Issac, B. Wittmann, M. Kivala, N. Hammer, J. Köhler, H.-W. Schmidt, R. Hildner, *Nature* **2015**, *523*, 196–199.
- [50] F. C. Spano, I. Introduction, *Acc. Chem. Res.* **2009**, *43*, 429–439.
- [51] N. J. Hestand, F. C. Spano, *Chem. Rev.* **2018**, *118*, 7069–7163.
- [52] U. Rösch, S. Yao, R. Wortmann, F. Würthner, *Angew. Chem. Int. Ed.* **2006**, *45*, 7026–7030.
- [53] D. M. Charron, G. Yousefalizadeh, H. H. Buzza, M. A. Rajora, J. Chen, K. G. Stamplecoskie, G. Zheng, *Langmuir* **2020**, *36*, 5385–5393.
- [54] O. P. Dimitriev, J. Zirzmeier, A. Menon, Y. Slominskii, D. M. Guldi, *J. Phys. Chem. C* **2021**, *125*, 9855–9865.
- [55] T. Brixner, R. Hildner, J. Kohler, C. Lambert, F. Würthner, *Adv. Energy Mater.* **2017**, *7*, 1700236.
- [56] S. Yagai, T. Seki, T. Karatsu, A. Kitamura, F. Würthner, *Angew. Chem. Int. Ed.* **2008**, *47*, 3367–3371.
- [57] N. Guo, H. You, Y. Song, M. Yang, K. Liu, Y. Zheng, *J. Mater. Chem.* **2010**, *20*, 9061–9067.
- [58] W. D. H. M. Yuan Yang, T. Wang, P. Yin, W. Yin, S. Zhang, Z. Lei, M. Yang, Y. Ma, *Mater. Chem. Front.* **2019**, *3*, 505–512.
- [59] Z. Wu, B. Tan, L. Gong, X. Zhang, H. Wang, Y. Fang, X. Hei, Z.-Z. Zhang, G. Zhang, X.-Y. Huang, J. Li, *J. Mater. Chem. C* **2018**, *6*, 13367–13374.
- [60] Z. Liu, Q. Tang, X. Li, T. Zhou, M. Liu, Y. Zhao, X. Lai, J. Bi, D. Gao, *J. Alloys Compd.* **2023**, *950*, 169877.
- [61] Q. Lin, P. Mao, L. Liu, J. Liu, Y. Zhang, H. Yao, T. Wei, *RSC Adv.* **2017**, *7*, 11206–11210.
- [62] I. O. Martins, F. Marin, E. Modena, L. Maini, *Faraday Discuss.* **2022**, *235*, 490–507.
- [63] H. Shao, J. Seifert, N. C. Romano, M. Gao, J. J. Helmus, C. P. Jaronec, D. A. Modarelli, J. R. Parquette, *Angew. Chem. Int. Ed.* **2010**, *49*, 7688–7691.
- [64] Z. Zhao, H. Zhang, J. W. Y. Lam, B. Z. Tang, *Angew. Chem. Int. Ed.* **2020**, *59*, 9888–9907.

Manuscript received: February 9, 2024
 Revised manuscript received: March 22, 2024
 Accepted manuscript online: March 25, 2024
 Version of record online: April 18, 2024